

LONG PRIMER EXTENSION BY A NOVEL INVERSE PCR METHOD

BY

C2009  
Stephanie Cara Bishop

Submitted to the graduate degree program in Biochemistry and Biophysics  
and the Graduate Faculty of the University of Kansas  
in partial fulfillment of the requirements for the degree of  
Master of Arts

---

Mark L. Richter, Ph.D.  
Chairperson

---

David O. Davido, Ph.D.

---

Stephen H. Benedict, Ph.D.

Date Defended: September 9, 2008

The Thesis Committee for Stephanie Cara Bishop certifies  
that this is the approved Version of the following thesis:

LONG PRIMER EXTENSION BY A NOVEL INVERSE PCR METHOD

Committee:

---

Mark L. Richter, Ph.D.  
Chairperson

---

David O. Davido, Ph.D.

---

Stephen H. Benedict, Ph.D.

Date Approved: April 8, 2009

## Table of Contents

	Page
Abstract.....	1
Abbreviations.....	2
List of Figures.....	3
List of Tables.....	4
Introduction.....	5
Materials and Methods.....	12
Results and Discussion.....	19
Conclusions and Implications for Further Research.....	35
References.....	39

## **Abstract**

An inverse polymerase chain reaction (PCR) was employed to construct an engineered  $F_1$ -ATPase by means of inserting the repressor of primer (Rop) DNA sequence into the region of the ATP synthase gamma ( $\gamma$ ) subunit DNA sequence encoding a regulatory dithiol-containing domain. A two-step PCR approach was developed to insert two unusually long (>100 base pairs each) primers encoding 189 base pairs of exogenous DNA into a single site within a pACYC multiple cloning host vector. The construct was verified by means of DNA sequencing. This approach allowed direct insertion of large pieces of DNA into a host DNA molecule without introducing restriction enzyme sites, thus avoiding common shortcomings such as inclusion or omission of base pairs that were associated with traditional sub-cloning methods. The engineered gamma subunit was designed for assembly with the recombinant alpha ( $\alpha$ ) and beta ( $\beta$ ) subunits into a core  $F_1$ -ATPase. The rigid twisted helical structure of the Rop protein extended the regulatory domain of the gamma subunit by approximately 60 Ångstroms, thus creating a rigid, rotating armature within the enzyme. The armature is intended for use as a site for attachment of gold particles to monitor rotation of the gamma subunit during ATP hydrolysis.

## Abbreviations

ADP: adenosine diphosphate

ATP: adenosine triphosphate

*atpC*: DNA sequence encoding the ATP synthase gamma subunit

BSA: bovine serum albumin

*E. coli*: *Escherichia coli*

F<sub>1</sub>: the membrane-associated portion of the ATP synthase complex, contains the catalytic domains and is comprised of subunits  $\alpha$ ,  $\beta$ ,  $\gamma$ ,  $\delta$ ,  $\epsilon$

F<sub>O</sub>: the membrane-embedded portion of the ATP synthase complex, is comprised of subunits a, b, c (I, II, III, and IV in the chloroplast F<sub>1</sub>)

GFP: green fluorescent protein

GTP: guanosine triphosphate

LB: Luria-Bertani Broth

PCR: polymerase chain reaction

P<sub>i</sub>: inorganic phosphate

Rop: repressor of primer

## Figures

Figure 1: Proposed structure of the ATP synthase complex.....	6
Figure 2: Gamma subunit rotation analysis.....	9
Figure 3: ATP-driven electrical generator.....	10
Figure 4: The protein Rop.....	13
Figure 5: Long primers Rop34gamma and Rop28gamma.....	15
Figure 6: Mitochondrial F <sub>1</sub> enzyme model.....	21
Figure 7: Agarose gel analysis of PCR products.....	33
Figure 8: Mutant atpCRop DNA sequence.....	34
Figure 9: atpCRop DNA sequence.....	36
Figure 10: SDS-PAGE analysis of gammaRop.....	37

## **Tables**

Table 1: Final PCR Conditions.....	31
------------------------------------	----

## Introduction

The adenosine triphosphate (ATP) synthase enzyme couples the transport of protons across the chloroplast or mitochondrial membrane to the synthesis of ATP from ADP and  $P_i$ . Subunits a, b, and c comprise the membrane-embedded proton-transporting  $F_o$  (factor O) portion of the enzyme complex. The  $F_1$  (factor 1) portion of the ATP synthase complex, peripheral to the membrane, contains the catalytic sites for ATP synthesis and hydrolysis. The  $F_1$  portion of the ATP synthase complex is comprised of the following subunits and stoichiometry:  $\alpha_3\beta_3\gamma_1\delta_1\epsilon_1$ . The proposed structure of the ATP synthase complex is presented in Figure 1 [1].

The  $\alpha$  and  $\beta$  subunits alternate to form the hexameric ring. One catalytic site is located on each  $\beta$  subunit, at the  $\alpha\beta$  interface; three non-catalytic sites exist on each  $\alpha$  subunit at the alternate  $\alpha\beta$  interfaces [2, 3]. The three, structurally asymmetric catalytic sites result from differential interactions between the  $\gamma$  subunit and each of the three  $\alpha\beta$  interfaces. Cooperative ATP binding, hydrolysis, and ADP release, during ATP hydrolysis, drives directional rotation of the  $\gamma$  subunit [2, 4, 5, 6]. The proton gradient drives rotation of the  $\gamma$  subunit in the direction opposite that of ATP hydrolysis; the catalytic sites work through the reverse series of conformational states, resulting in high-affinity binding of ADP and  $P_i$ , ATP synthesis, and then ATP release [4, 6, 7, 8]. While ATP synthesis requires a proton gradient and the entire complex, the core catalytic  $F_1$  portion, comprised of  $\alpha$ ,  $\beta$ , and  $\gamma$  subunits, is sufficient for ATP hydrolysis.

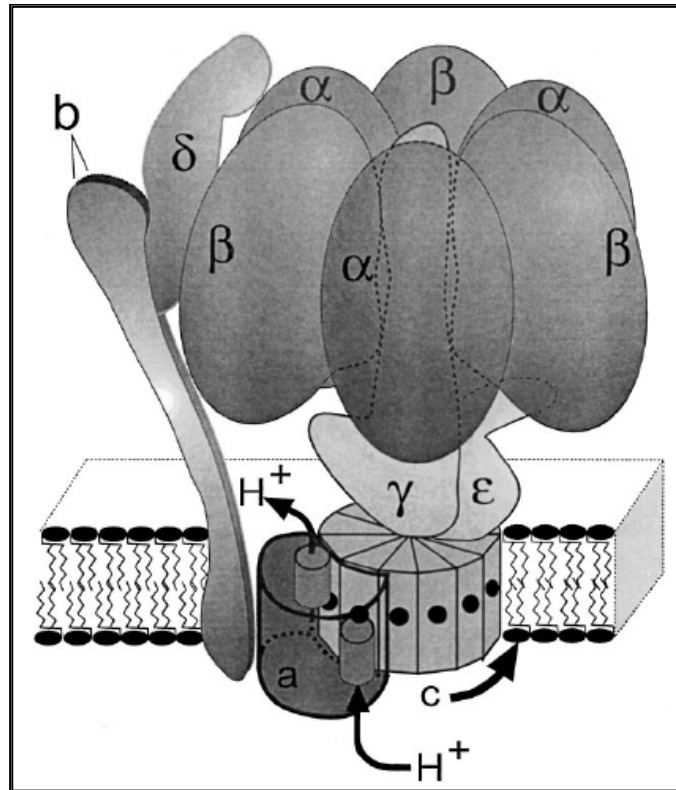


Figure 1: Proposed structure of the ATP synthase complex [1]. Subunits a, b, and c comprise the F<sub>O</sub>, or membrane-embedded portion; subunits  $\alpha$ ,  $\beta$ ,  $\gamma$ ,  $\delta$ ,  $\epsilon$  comprise the F<sub>1</sub>, or membrane-associated portion. ATP is synthesized through an as yet uncharacterized mechanism when protons cross the membrane through the enzyme complex, down the concentration gradient. Used for educational purposes, without permission, from [1].

A great deal of research has centered on quantitation of the kinetics of rotation of the  $\gamma$  subunit within the  $F_1$  complex to drive ATP synthesis and hydrolysis [9 – 13]. To accomplish this, researchers have employed protein engineering approaches [9, 10, 13, 14, 15] to attach the  $\alpha\beta$  hexameric ring to a rigid substrate and to modify the  $\gamma$  subunit in order to observe its rotation within the  $\alpha\beta$  hexamer. Typically, a biotin-streptavidin linker was covalently attached to a cysteinyl residue introduced at the top of the  $\gamma$  subunit and an actin filament [9], nickel rod [14], gold rod [15], or gold bead [10] was attached to the streptavidin. Fluorescence or dark-field microscopy was then used to analyze rotation. The most definitive experiment in terms of quantitating gamma subunit rotation was that shown in Figure 2, in which a gold bead of approximately 40 nm in diameter was attached to the  $\gamma$  subunit as indicated. From this experiment, researchers suggested that the  $\gamma$  subunit rotated in discrete  $120^\circ$  steps. Apparent pauses (or sub-steps) in bead rotation of  $\sim 90^\circ$  and  $\sim 30^\circ$  could also be resolved under some conditions [10], although the presence, size, and nature of these pauses is controversial.

A significant problem with these experiments is that the resolution of the stepping action was limited by the superposition of the rotating bead directly on top of the enzyme's center of axis of rotation. Thus, the bead displacement from the rotating axis was, at best, only a few Ångstroms, making it difficult to determine if the bead rotated uniformly in a single direction. In addition, the Brownian motion associated with the attached rods or beads had not been evaluated, leaving further questions about whether or not the enzyme seen in dark-field microscopy studies,

especially under conditions of limiting substrate when the catalytic rate was very small, actually rotated, or merely oscillated as a result of Brownian motion. It is of considerable importance to properly resolve the stepping and sub-stepping action of the gamma protein and to relate these steps to specific protein-protein and nucleotide-protein interactions within the enzyme complex. This will provide the necessary information to resolve the mechanism by which this remarkable enzyme captures the energy from ATP hydrolysis and converts it into rotational torque. In addition to characterizing the enzyme's rotational mechanism, the rotary action of the ATP synthase complex can be used in multiple nanodevice applications that require conversion of chemical energy into kinetic motion. For example, coupling F<sub>1</sub> enzyme ATP hydrolysis-driven rotation to produce electricity by means of fabricating a nano-sized rotary engine is a platform from which many new applications can be launched. Such a device, depicted in Figure 3, is one of the principle future goals of this work.

In the device shown in Figure 3, the hybrid  $\gamma$ , in the center of the surface-attached F<sub>1</sub> molecule, has an extended armature, shown in cyan, which is comprised of the engineered Rop protein. The F<sub>1</sub> complex, comprised of alternating  $\alpha$  (red) and  $\beta$  (blue) subunits, is attached to a rigid substrate. A magnetic bead (brown) is shown attached to the tip of the Rop armature. ATP hydrolysis will elicit  $\gamma$  subunit rotation and the magnetic bead will pass over a series of nano-sized electrodes (yellow) that will have been etched into the substrate surface using electron beam lithography. As the bead passes over the electrodes, a nanowatt electrical current is expected to be generated.

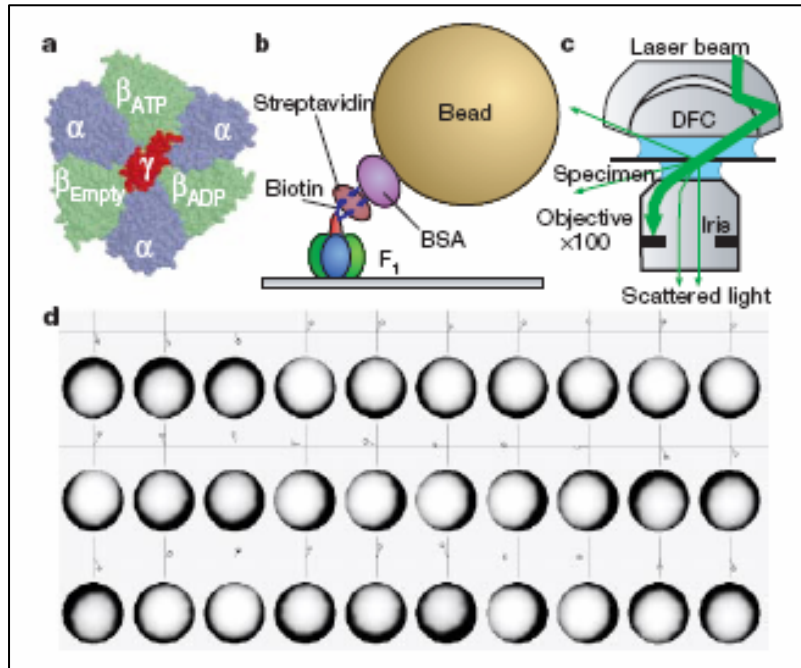


Figure 2: Gamma subunit rotation analysis [10]. The ATP synthase complex  $F_1$  portion subunits  $\alpha$  (blue),  $\beta$  (green), and  $\gamma$  (red) are presented (a) with the nucleotide binding site occupant indicated (ATP, ADP, or empty). Panel b illustrates the biotin-streptavidin-BSA linkage that was used to join the gold bead to a cysteine residue engineered into the tip of the  $\gamma$  subunit (red). Subunits  $\alpha$  (blue) and  $\beta$  (green) were attached to a rigid substrate via poly-Histidine tags employed to observe rotation of the gold bead around the immobilized  $\alpha\beta$  hexameric ring. Panel d shows images of a gold bead at different times (ms) during ATP-driven rotation relative to a fixed circle. Used for educational purposes, without permission, from [10].

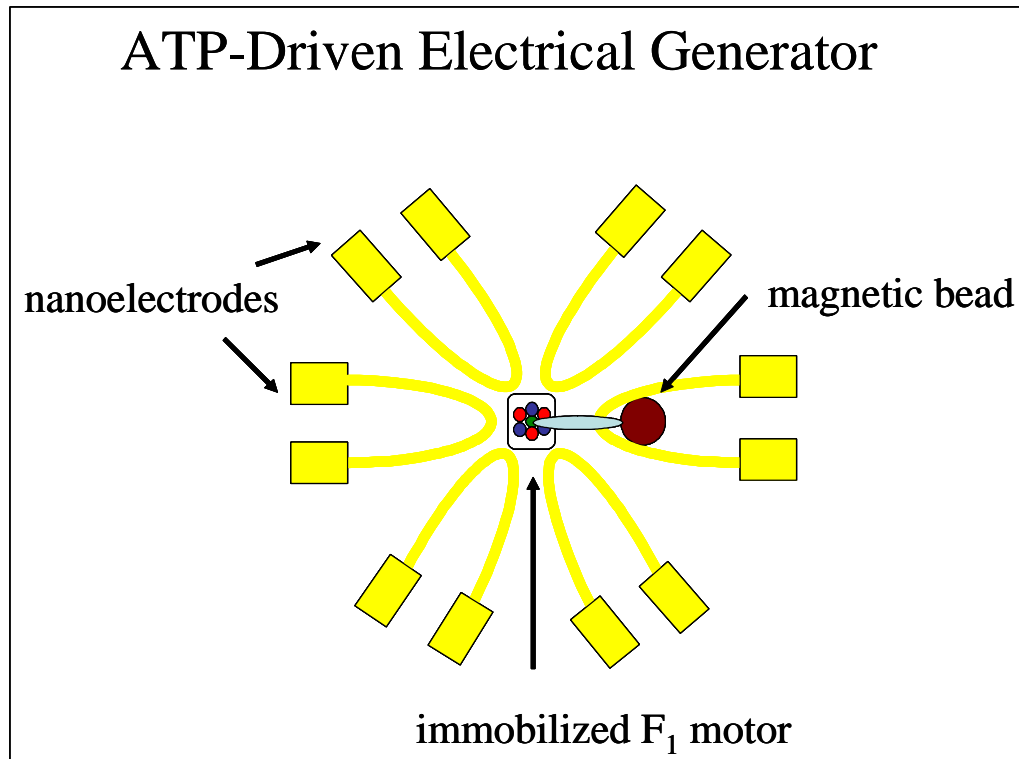


Figure 3: ATP-driven electrical generator. The hybrid gamma subunit, in the center of the surface-attached  $F_1$  molecule, has an extended armature shown in cyan that is comprised of the engineered Rop protein. The  $F_1$  complex, comprised of alternating  $\alpha$  (red) and  $\beta$  (blue) subunits, is attached to a rigid substrate. To the tip of the Rop armature will be attached a magnetic bead (brown). ATP hydrolysis will elicit gamma subunit rotation and the magnetic bead will pass over a series of nano-sized electrodes (yellow) that have been etched into the substrate surface using electron beam lithography. As the bead passes over the electrodes, a nanowatt electrical current is expected to be generated.

Here, we describe experiments in which a long primer inverse PCR extension method was used to introduce a rigid armature into the rotating gamma subunit that we predict, from molecular models of the gamma subunit, will extend the radius of rotation of attached particles, such as metallic beads, by approximately 60 Ångstroms. This is expected to provide significantly greater resolution of the enzyme's rotational steps and sub-steps in dark-field microscopy experiments and it will also serve as the first phase in developing the nanodevice shown in Figure 3. The experiments involved genetic insertion of the DNA sequence of a rigid, helical protein, Rop (repressor of primer), into the dithiol-containing domain of the photosynthetic gamma ATP synthase subunit. Originally characterized in 1982 [16], Rop is a regulatory protein involved in plasmid DNA replication. It modulates transcription initiation of the primer RNA precursor [17]. The 189 base pair *rop* DNA sequence encodes Rop, a 63 amino acid twisted, rigid  $\alpha$ -helical protein, illustrated as a dimer in Figure 4 [18]. The monomeric, twisted helical structure is expected to be rigid and highly stable.

There are a number of issues associated with insertion of long pieces of DNA into a host DNA molecule. For example, typical sub-cloning methods, i.e. introducing restriction sites into the two DNA fragments, may necessitate introducing or deleting nucleotides from the host DNA or DNA insert. In addition, successful ligation is often stymied by difficulty obtaining the correct ratio and the correct orientation of the insert. Inverse PCR is commonly used for the introduction of nucleotide changes or for the insertion of small lengths of exogenous DNA into a

gene or vector [19, 20]. It can also be used to delete >100 base pairs of a gene of interest with higher deletion efficiency than the overlapping primer method [21].

Long primer PCR, the method used in this study, offers several advantages over traditional methods of insertion of long pieces of exogenous DNA. This technique avoids problems with restriction digestion of DNA, ligating insert DNA into the template, and ensuring that the ligated product contains 1) the sequence of interest in the proper insert:vector ratio and 2) the proper orientation of the inserted DNA sequence. While amplification of long targets (10 – 40 kb) has previously been demonstrated [22], we describe the successful insertion and amplification of 189 bases of foreign DNA, introduced by “long primers”.

## **Materials and Methods**

### **Sub-Cloning**

The DNA encoding the spinach chloroplast ATP synthase gamma subunit (*atpC*) was previously sub-cloned into the pET8cgam bb1 vector [23]. The pACYCatpC vector was prepared by inserting the chloroplast ATP synthase gamma subunit DNA sequence into the NcoI multiple cloning site of the pACYC Duet Coexpression Vector (71147-3, Novagen, San Diego, CA). This insertion was accomplished by restriction digestion of the gamma subunit N-terminus with NcoI (Promega, Madison, WI) and of the C-terminus with BamHI (Promega) and a simultaneous restriction digestion of the pACYC Duet Coexpression Vector. The DNA sequence and apparent molecular weight of the expressed protein were obtained

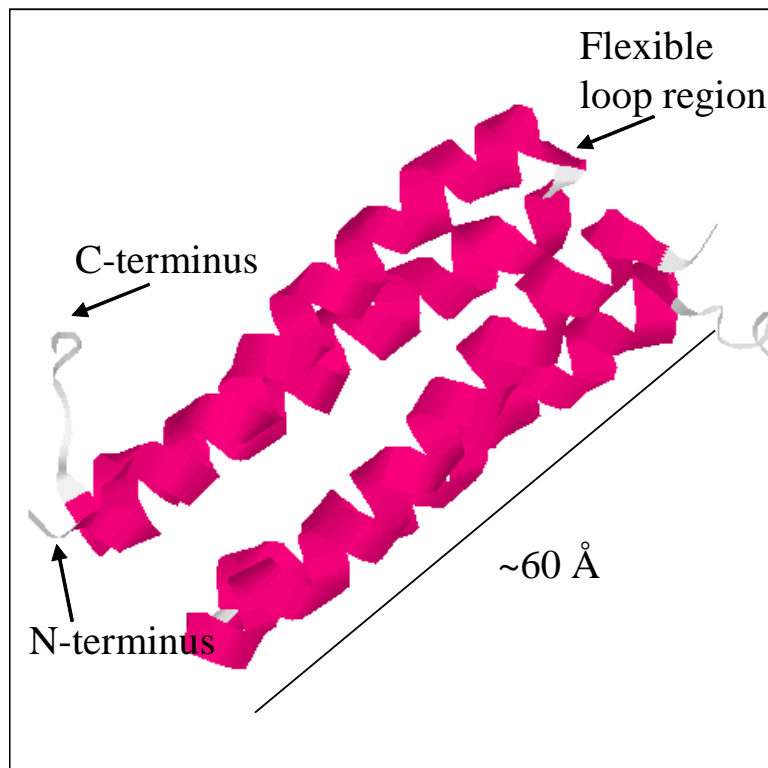


Figure 4: The protein Rop, shown as a dimer, modified from PDB 1RPR [18] using Rasmol. The helical, coiled-coil protein is approximately 60 Å long and contains a flexible loop region between the two helices. The flexible loop region is the proposed location for the insertion of a cysteine residue for covalent attachment of a gold bead for rotation studies similar to those described in Figures 2 and 3.

by means of DNA sequencing and SDS-PAGE, respectively, to ascertain that the gamma subunit DNA sequence had been incorporated in the correct orientation, in the proper location, within the pACYC Duet Coexpression Vector.

### **Long Primer Extension**

For purposes of primer design, the Rop DNA sequence was obtained from PubMed, NCBI J01749 [18]. Primers were designed to insert the entire Rop DNA sequence (189 bases) between atpC amino acids 223 (lysine) and 224 (leucine). Unphosphorylated long primers (Integrated DNA Technologies, Coralville, IA) had the following sequences:

Rop28gamma: 5'CAG TTC GTT GAG CTT CTC CAG CAG CGT TAA TGT CTG  
GCT TCT GAT AAA GCG GGC CAT GTT AAG GGC GGT TTT TTC CTG TTT  
GGT CTT ACC TTC TTT TGT TGT GAG 3'

Primer Rop28gamma contained the DNA sequence for the N-terminal half of Rop in addition to 21 bases (underlined) of the ATP synthase gamma subunit DNA sequence (Figure 5).

Rop34gamma: 5'GAC GCG GAT GAA CAG GCA GAT ATC TGT GAA TCG CTT  
CAC GAC CAC GCC GAT GAG CTT TAC CGC AGT TGC CTC GCT CGC TTC  
GGG GAT GAC GGT GAA AAC CTC CTA ACG GTA GAA AGA GAC ATG 3'.

Primer Rop34gamma contained the DNA sequence for the C-terminal half of Rop in addition to 21 bases (underlined) of the ATP synthase gamma subunit DNA sequence (Figure 5). Primers Rop28gamma and Rop34gamma were evaluated for the

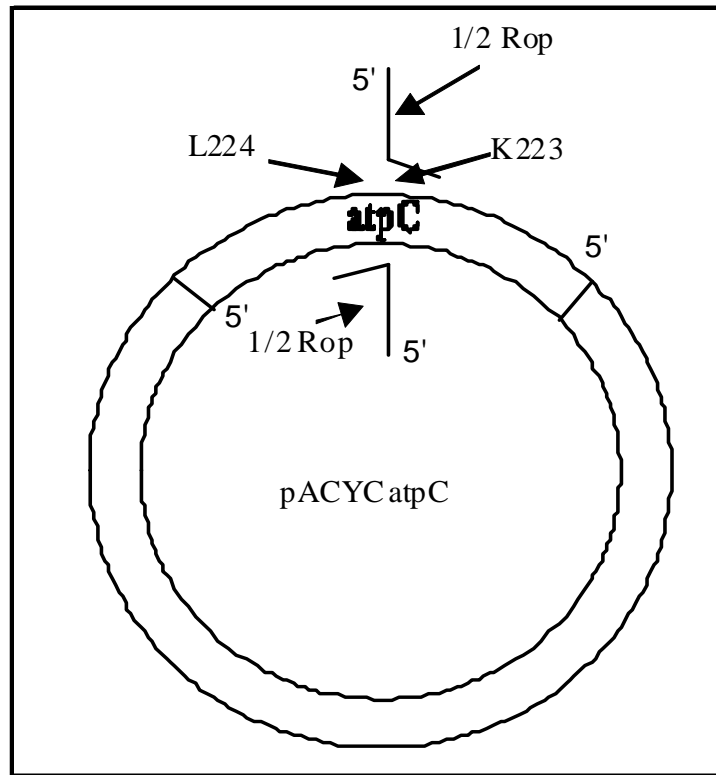


Figure 5: Long primers Rop34gamma and Rop28gamma and their alignment with vector pACYCatpC. Each long primer anneals to 21 bases of the *gamma* DNA sequence and contains approximately half of the *rop* DNA sequence. The long primer PCR using these primers generates a linear, blunt-ended product approximately 5.5 kb in length (4.3 kb plasmid, 1 kb *gamma*, 0.2 kb *rop*).

propensity to form hairpins, self-dimers, or hetero-dimers, using IDT's online OligoAnalyzer SciTool (Coralville, IA). Primers contained no known restriction enzyme digestion sites. The approximate percent GC content of ~50% was also within the acceptable limit of <60%.

*PfuUltra* High-fidelity DNA Polymerase and buffer, (600380, Stratagene, La Jolla, CA), dNTPs, (Promega, Madison, WI), and GoTaq® Flexi DNA Polymerase, (M8291, Promega) were employed in the inverse polymerase chain reaction using two unique annealing temperatures and durations (57°C for 30 seconds; 68°C for 10 minutes). Gel purification was performed, according to manufacturer's specifications, using Qiaquick® Gel Extraction kit (28704, Qiagen Sciences, Valencia, CA). The gel-purified, linear, 5.5 kilobase PCR product was treated with T4 Polynucleotide Kinase (69248-3, Novagen, San Diego, CA) according to manufacturer's specifications. After treatment, the kinase was inactivated by incubation at 70°C for 10 minutes.

### **Ligation**

T4 DNA Ligase (M0202T, New England Biolabs, Ipswich, MA) was used for blunt-end ligation of linear PCR products. T4 Polynucleotide Kinase (Novagen) was incorporated into the ligation tube. Chloramphenicol (C-0378, Sigma Chemical, St. Louis, MO) was used at 34 µg/mL final concentration for *E. coli* bacterial growth in suspension and on agar plates.

## **Transformation**

High-efficiency transformation was completed using New England Biolabs 5- $\alpha$ F'I<sup>q</sup> competent cells (C2992I, Ipswich, MA), according to manufacturer's specifications with chloramphenicol on Luria-Bertani Broth (LB) plus agar plates. Cells were incubated overnight at 37°C with 5% CO<sub>2</sub> in a humidified chamber. To evaluate transformants, colonies were incubated in 1 mL LB medium supplemented with chloramphenicol in a rotating incubator at 250 rpm at 37°C until the medium became cloudy (approximately 4.5 hours). After growth, 5  $\mu$ L of cell suspension and 45  $\mu$ L water were heat-denatured at 95°C for 30 minutes. Cell stocks in DMSO were prepared by adding the remaining volume (~1 mL) of cell suspension to 80  $\mu$ L DMSO (Fisher Scientific) and frozen at -80°C. Transformants were characterized by means of PCR using the following sets of primers (Integrated DNA Technologies, Coralville, IA):

Gamma F 5' T ACT TCC AAT CCA ATG GCA AAC CTC CGT GAG CTA 3'

Gamma R 5' T TAT CCA CTT CCA ATG TCA AAC ACA TGC ATT AGC 3'

Rop F 5'GAG GCA CCA TGG ACC AAA CAG GAA 3'

Rop R 5'GAG CTG CAT CCA TGG GAG GTT TTC ACC 3'

## **Plasmid Preparation**

*Escherichia coli* bacteria containing the pACYCatpCRop plasmid were grown at 37°C in a rotating incubator at 250 rpm overnight. Plasmid preparation was performed according to Qiaprep® Spin Miniprep (27104, Qiagen, Valencia, CA) instructions, except that DNA was eluted with water, not EB buffer. DNA

concentrations were determined using a Cary Win UV/Vis spectrophotometer and a 1-cm path length quartz cuvette at a wavelength of 260 nm against water (blank). DNA sequencing was performed at The Iowa State DNA Sequencing Facility (Ames, Iowa). Agarose gels were prepared with ethidium bromide and visualized via UV light. A 10 kilobase DNA hyperladder (Biolone, Taunton, MA) was incorporated in all agarose gel analyses.

### **Protein Expression**

The pACYCatpCRop plasmid was transformed into BL21DE3pLys competent cells (70236 Novagen, San Diego, CA) according to manufacturer's specifications. *Escherichia coli* BL21DE3pLys bacteria containing the pACYCatpCRop plasmid were grown at 37°C in a rotating incubator at 250 rpm overnight. After overnight incubation, the cells were transferred to 2 L of LB medium containing antibiotics and grown at 37°C in a rotating incubator until the O.D. reached ~0.6 at 600 nm. Once the culture reached the appropriate optical density, the culture was induced with IPTG at a final concentration of 40 mM. The culture was incubated at 15°C in a rotating incubator overnight. After incubation, the culture was centrifuged at 3000 x g for 5 minutes at room temperature. The supernatant fluid was discarded and the pellet was resuspended in water. The cells were subjected to sonication and freeze/thaw lysis after which time the pellets were resuspended and stored in 50 mM Tris/2 mM EDTA, pH 8.0. Cell lysates were analyzed by means of SDS-PAGE and Coomassie staining.

## Results and Discussion

A recently-constructed model of the  $\gamma$  subunit of the photosynthetic ATP synthase [24, 25] was used to predict the position for the Rop insertion that was expected to result in maximum extension of the  $\gamma$  regulatory domain in a direction approximately perpendicular to that of the axis of rotation. The model is shown in Figure 6. The regulatory domain extended from residues 196 to 242 and included the disulfide-forming thiols at positions 199 and 205, as indicated in yellow. Extensive mutations had been performed within the regulatory domain [26] and indicated that the entire domain or large sections of the domain could be removed without decreasing the maximum catalytic rate of the enzyme. Most mutants exhibited loss of the inhibition that was imposed on catalytic turnover by formation of the disulfide bridge between cysteine residues 199 and 205. The insensitivity to mutation on this part of the gamma subunit made it a good choice for insertion of the Rop protein. The Rop DNA sequence was inserted in the *gamma* gene between lysine residue 223 and leucine residue 224 (shown as threonine 224), as indicated in Figure 6. The model predicted that this would extend the regulatory domain approximately 60 Å from the center of axis of rotation.

### Summary of Unsuccessful Cloning Attempts

Initially, a traditional sub-cloning procedure was employed to generate the desired genetic construct. The pET8cgam bb1 vector, containing the *atpC* DNA sequence, was modified using primers for site-directed mutagenesis to introduce an

NcoI restriction enzyme digestion site between amino acids lysine 223 and leucine 224. An amplified, purified Rop DNA sequence fragment was obtained using Rop (F) and Rop (R) primers and the pBR322 plasmid, which contained the *rop* DNA sequence. The pET8cgamma vector and the purified Rop DNA fragment were restriction enzyme digested with NcoI. Ligation of the digested fragment into the pET vector was attempted by varying the ratio of insert:vector, ligation duration and temperature, and ligase enzyme concentration. Ligated constructs were transformed into XL1Blue high-efficiency cloning cells; transformants were evaluated by means of PCR and subsequent agarose gel analysis. Polymerase chain reactions were performed using Rop (F), Rop (R), gamma (F), and/or gamma (R) primers. Gel analysis of the PCR products revealed several problems. A portion of the N-terminus of the gamma subunit was absent. Polymerase chain reaction amplification using Rop (F) and Rop (R) primers generated a very dense, sharp band at 200 base pairs for nearly all transformants, but amplification using gamma (F), gamma (R) primers did not generate a band for the same transformants. Multiple attempts at generating the desired genetic construct indicated that there was an inadvertent NcoI restriction digestion sequence at the N-terminus of the gamma DNA sequence, thereby explaining the absence of PCR product when the gamma primers were used. It was also discovered that the pET vectors contain an endogenous *rop* DNA sequence, thereby explaining the presence of a dense, 200 base pair band for all transformants. Finally, it was discovered that the *gamma* DNA sequence contained an inadvertent BamHI restriction site within its N-terminus.

## Engineering an Extended Arm into the $F_1 \gamma$ Subunit

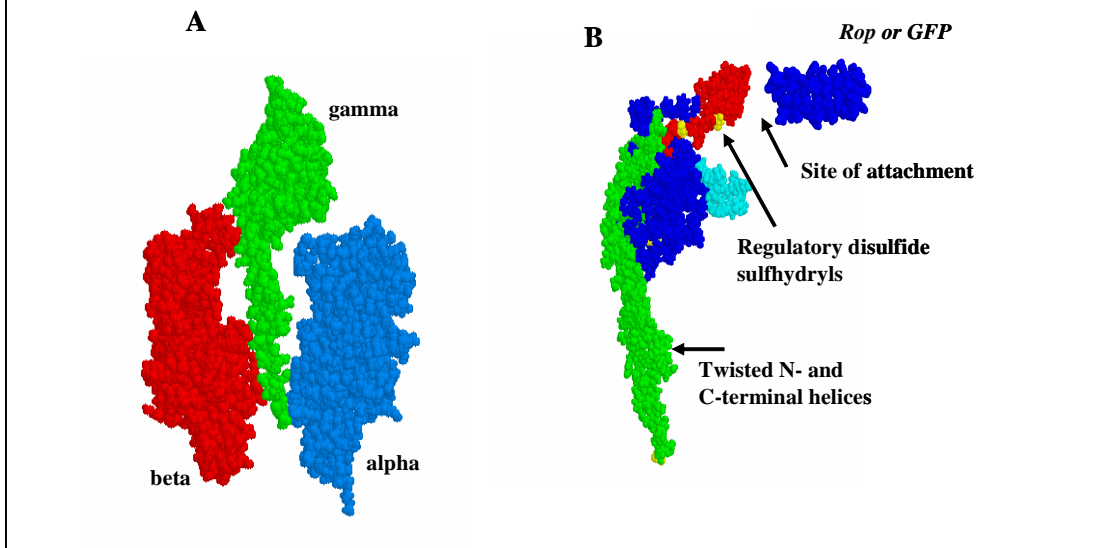


Figure 6: Panel A shows a cross-section through the crystal structure of the mitochondrial  $F_1$  enzyme and indicates the position of the gamma subunit. Panel B shows the predicted structure of the chloroplast  $F_1$  gamma subunit indicating where the *Rop* insertion will be made. The regulatory dithiol-containing domain of the chloroplast gamma subunit (red in Panel B) is not present in the mitochondrial enzyme and can be completely deleted from the chloroplast enzyme without loss of catalytic function [23]. The *rop* (or *gfp*) DNA sequence has been spliced directly into the regulatory, dithiol-containing domain of the chloroplast gamma subunit.

To overcome these obstacles, site-directed mutagenesis was performed to mutate the NcoI restriction enzyme digestion site to an NdeI restriction enzyme digestion site and to alter the inadvertent BamHI site. In addition, the *atpC* DNA sequence was restriction digested with NdeI, at the N-terminus, and BamHI, at the C-terminus and ligated into the pTBSG vector [Fei Gao, unpublished], which contained the tobacco etch virus (TEV) and maltose binding protein (MBP) DNA sequences. The pTBSG vector contained DNA sequences for TEV and MBP to facilitate purification and solubility during protein expression, which was particularly important given that the Rop protein was involved in primer repression and its expression resulted in poor plasmid replication and poor colony growth. Ultimately, the gamma-Rop-gamma genetic construct was generated within the pTBSG vector. This vector, however, contained an endogenous Rop sequence. To obtain large quantities of the desired construct and to minimize the formation of Rop homodimers during protein expression, it would have been necessary to excise the band of interest and re-clone it into an alternative vector, such as the pACYC Duet Coexpression Vector. Because the pACYC Duet Coexpression Vector contained two unique multiple cloning sites and did not contain an endogenous *rop* DNA sequence, it was the desired plasmid for this application. While attempts at generating the desired construct using this approach were ongoing, other approaches were initiated to maximize the likelihood of success.

One alternative approach attempted to generate the desired genetic construct using existing sets of primers in unique combinations. Prior to PCR, T4

polynucleotide kinase was used, according to manufacturer's specifications, to phosphorylate aliquots of the >100 base pair, "long primers" Rop28gamma and Rop34gamma, which each contain half of the *rop* DNA sequence and anneal to 21 bases of the *gamma* DNA sequence in the pACYCatpC expression plasmid (Figure 5). The PCR reaction was performed using primer gamma (F) in addition to primer Rop28gamma in one tube and primer Rop34gamma in addition to primer gamma (R) in a second tube. The pACYCatpC vector was employed as template in both reactions. The PCR product from the first tube was the N-terminal half of gamma plus the N-terminal half of Rop (Ngamma-Rop). A PCR amplification reaction of the second tube generated the C-terminal half of Rop plus the C-terminal half of gamma (Rop-Cgamma). Products were visualized on ethidium bromide-containing agarose gels. The PCR products were gel-purified and subjected to ligation at varying ratios of Ngamma-Rop and Rop-Cgamma DNA fragments and varying amounts of T4 DNA Ligase. Ligated products were evaluated by agarose gel electrophoresis and subjected to gel purification. Attempts to obtain appropriately-sized PCR products after PCR optimization were unsuccessful. Attempts to obtain ligated constructs with the appropriate orientation were not ameliorated by attempts to re-phosphorylate PCR products generated using phosphorylated primers, or by phosphorylating PCR products generated using unphosphorylated primers.

Attempts to generate the gammaRopgamma genetic construct using traditional cloning techniques were eventually abandoned due to difficulties obtaining the desired ligated product and difficulty interpreting PCR products due to the presence

of false positives resulting from the endogenous *rop* DNA sequence contained within the pET vector. Attempts to generate the gammaRopgamma construct using the Ngamma-Rop and Rop-Cgamma approach were abandoned due to difficulties obtaining and ligating appropriately-sized PCR products. In spite of the effort placed on this approach, the desired genetic construct was not obtained and a third method was initiated.

### **Examining a long-primer extension approach**

“Long primer” or inverse PCR was employed in an attempt to generate a plasmid containing the foreign DNA of interest, inserted into a specific location in the host DNA molecule, using 105 and 123 nucleotide long primers indicated in the Materials and Methods section. With inverse PCR, the foreign DNA is introduced via “long primers” or primers greater than 100 bases in length; each primer contains ½ of the DNA sequence of the foreign insert. The PCR product is linear and must be blunt-end ligated prior to transformation.

In an attempt to generate the gammaRopgamma genetic construct using the long primer extension approach, traditional PCR conditions were employed. This set of PCR conditions did not result in a product visible by means of agarose gel electrophoresis. To improve annealing of GC-rich regions, 5% DMSO was added to the PCR reaction tubes. PCR was repeated using phosphorylated Rop34gamma and Rop28gamma in one tube and unphosphorylated Rop34gamma and Rop28gamma primers in a separate tube. A gradient thermocycler program was used to determine optimal annealing temperature. PCR was repeated, using the optimized annealing

temperature, to determine the optimal magnesium chloride concentration. Many PCR reactions were attempted, using purified primers with and without T4 polynucleotide kinase treatment, 5% DMSO, and DpnI digestion. In addition, different primer concentrations, template concentrations, and polymerase sources and concentrations were tried.

PCR was repeated using two unique annealing temperatures, the first at 52°C and the second at 68°C. The first annealing temperature corresponded to annealing between the 21 base pairs of the *gamma* DNA sequence on the Rop34gamma primer or the Rop28gamma primer to the *gamma* DNA sequence within the plasmid. The second annealing temperature corresponded to annealing between the Rop34gamma primer or the Rop28gamma primer and the product of the first annealing and elongation steps. The second annealing temperature was greater than that of the first annealing temperature because greater than 21 base pairs anneal during this phase. The product of the first annealing and elongation presented an opportunity for a greater number of base pairs to anneal between primers Rop34gamma or Rop28gamma and the product. Optimal long primer inverse PCR required an initial round (step one) with low annealing temperature and short annealing duration because primers were required to anneal to approximately 21 bases of the gamma subunit sequence. During the second PCR step, the annealing temperature and duration were increased significantly because the primers were annealing to a DNA sequence that was complementary to the entire primer length (>100 base pairs).

This set of PCR conditions generated a 5.5 kb band, but attempts at ligation and transformation were unsuccessful. PCR was repeated using variable polymerase concentrations. The final, 50  $\mu$ L volume was divided into 2 tubes of 25  $\mu$ L each, prior to initiating the PCR program because it was noted that smaller reaction volumes efficiently undergo the temperature changes required by this PCR program.

In the process of PCR optimization, it was noted that while Stratagene *Pfu Ultra* polymerase mixes appeared similar according to manufacturer's specifications sheets, only *Pfu Ultra* 600380-51 consistently gave a dense, sharp band at 5.5 kb. For each PCR reaction, each *Pfu* polymerase enzyme was accompanied by its corresponding 10x Buffer, for example, *Pfu* polymerase 600380-51 was accompanied by its 10x Buffer 600380-52. To optimize PCR, template quantity, primer quantity, enzyme activity, polymerase source and supplier, and magnesium chloride concentration were all varied. In addition, the PCR conditions were varied, including cycle number, melting, annealing, and elongation temperatures and durations, before optimal conditions were determined.

Ligation was attempted using T4 DNA Ligase and buffer using varying concentrations of DNA. Ligation was optimized using variable amounts of PCR products that were purified, phosphorylated, and re-phosphorylated. Variable ligation temperatures, durations, enzyme and buffer suppliers, and enzyme activities were employed prior to achieving blunt-end ligation of the linear PCR product pACYCatpCRop.

Transformation was also attempted using different high-efficiency cloning competent cells and variable ratios of DNA:cells. A variety of transformation conditions were employed, including variable 0°C incubation durations, amount and duration of SOC medium addition and incubation, and culture temperature variations (37°C, 22°C, or 15°C) and durations. Transformation into XL1Blue high-efficiency cloning competent cells (Novagen) generated only small colonies only after an extended growth period (~20 hours at 37°C).

Many attempts to transform the ligated construct into XL1Blue, high-copy number competent cells (Novagen 70181) were unsuccessful. Close inspection of the tubes containing the competent cells indicated that there were non-uniform portions of competent cells frozen to the sides and lids of the microcentrifuge tubes, as if these fragile cells had been handled harshly or had been through a freeze/thaw cycle prior to arrival. Multiple shipments of these cells arrived, all appearing as if the cells had been handled roughly. Numerous attempts at transforming the construct failed and competent cells from a different supplier were investigated.

Five- $\alpha$ F'I<sup>q</sup> high-efficiency cloning competent cells (New England Biolabs, C2992I) were obtained and inspected prior to transformation. Cells were uniformly pelleted at the bottom of the microcentrifuge tube, indicating that the cells may have been handled more gently and/or may not have undergone a freeze/thaw cycle prior to arrival. While additional attempts to transform the pACYCatpCRop plasmid into XL1Blue competent cells may have eventually been successful, transformation of the genetic construct into 5- $\alpha$ F'I<sup>q</sup> high-efficiency cloning competent cells following

manufacturer's specifications, was successful after many fewer transformation attempts.

Finally, multiple transformation attempts employed variable incubation temperatures and durations, different competent cell suppliers, and different ratios of DNA:competent cells prior to successfully transforming the pACYCatpCRop construct into 5- $\alpha$ F<sup>1</sup> high-efficiency cloning competent cells.

### **The Final Cloning Strategy**

The “long-primer” or “inverse” polymerase chain reaction method was further modified to generate the desired genetic construct. The 105-nucleotide and a 123-nucleotide long primers, Rop28 $\gamma$  and Rop34 $\gamma$ , respectively, each containing the nucleotide sequence of approximately half of the *rop* gene, was obtained from Integrated DNA Technologies (Coralville, IA). Aliquots of long primers Rop28 $\gamma$  and Rop34 $\gamma$  were phosphorylated prior to PCR, thereby removing the need to phosphorylate the PCR product using T4 polynucleotide kinase. Alternatively, unphosphorylated primers Rop28 $\gamma$  and Rop34 $\gamma$  were used in the PCR reaction and the PCR product was subsequently phosphorylated using the T4 polynucleotide kinase.

The inverse PCR conditions listed in Table 1, “Final PCR Conditions”, generated a sharp 5.5 kb product with little non-specific binding, which was visualized using agarose gel electrophoresis (data not shown). After gel extraction and treatment of the 5.5 kb PCR product with T4 polynucleotide kinase, agarose gel

electrophoresis of a small aliquot of PCR product confirmed the presence of the expected 5.5 kb product (data not shown).

Blunt-end ligation of linear PCR products was achieved using T4 DNA Ligase (M0202T, New England Biolabs, Ipswich, MA) at a final activity of  $2 \times 10^6$  mU/ $\mu$ L; T4 Polynucleotide Kinase (Novagen) was incorporated into the ligation tube at a final activity of 1 U/ $\mu$ L. Ligation was carried out at room temperature for 4 hours then at 16°C overnight. Chloramphenicol was used at 34  $\mu$ g/mL final concentration for *E. coli* bacterial growth in suspension and on agar plates.

Ligation of linear pACYCatpCRop was confirmed by PCR using primers gamma (F) and gamma (R) (data not shown). The PCR product, visualized on an agarose gel, had a single band at 1.2 kb; no band was present at 1 kb, indicating the absence of contaminating pACYCatpC template.

Transformation of ligated pACYCatpCRop into 5- $\alpha$ F'I<sup>d</sup> high-efficiency cloning competent cells (New England Biolabs) generated many transformants after typical overnight (~12-16 hours) incubation at 37°C. Transformants were evaluated after heat denaturation using PCR with primers gamma (F) and Rop (R). Gel electrophoresis analysis indicated a band at the expected size of 800 base pairs, corresponding to amplification of the DNA sequence analogous to the N-terminus of gamma to amino acid L223 (~700 base pairs) and approximately half of the Rop DNA sequence (~100 base pairs) (data not shown). The presence of this 800 base pair PCR product indicated not only that both gamma and Rop were present, but also that they were in the appropriate orientation.

Additional verification of the transformant was carried out after plasmid preparation. Because of rapid bacterial growth and a high concentration of plasmid, the pACYCatpCROp plasmid did not likely interfere with plasmid replication. Using gamma (F) and gamma (R) primers and the plasmid pACYCatpC template as a positive control, gel analysis indicated a 1 kb PCR product. Using gamma (F) and gamma (R) primers and the plasmid pACYCatpCROp template, gel analysis indicated a 1.2 kb PCR product. A 200 bp PCR product was generated using Rop (F) and Rop (R) primers and pACYCatpCROp as template (Figure 7).

These results indicated that the pACYCatpCROp plasmid contained both the N- and C- termini of the ATP synthase gamma subunit DNA sequence and the Rop DNA sequence. Finally, DNA sequencing (Iowa State DNA Sequencing Facility, Ames, Iowa) confirmed the successful manufacture of the pACYCatpCROp construct using the newly developed long primer inverse polymerase chain reaction.

The DNA sequence of the putative atpCROp sequence within the plasmid, Figure 8, contained an extra guanosine triphosphate (GTP) nucleotide in the middle of the Rop sequence, where primers Rop28gamma and Rop34gamma meet. The inadvertent inclusion of this extra base resulted in a truncation mutation, whereby a protein approximately half of the expected size was expressed, purified, and visualized on an SDS-PAGE gel (data not shown). With the exception of the extra GTP nucleotide within the pACYCatpCROp plasmid, no other mutations existed. Both primers Rop28gamma and Rop34gamma contained the GTP nucleotide at their 3' ends. For these reasons, it was suspected that the one of

<u>Component</u>	<u>Final Concentration*</u>	<u>Step</u>	<u>Temperature</u>	<u>Duration</u>
Water	n/a	1	95 °C	30 sec.
10x <i>Pfu</i> Ultra HF reaction buffer	1x	2	94 °C	30 sec.
dNTPs, 10 mM each	0.2 mM each	3	57 °C	30 sec.
Rop34γ, 10 μM	0.2 μM	4	72 °C	6 min.
Rop28γ, 10 μM	0.2 μM	5	Go to 2	Rep 10
pACYCatpC, 96 ng/μL	1.92 ng/μL	6	94 °C	30 sec.
<i>Pfu</i> polymerase, 2.5 U/μL	50 mU/μL	7	68 °C	10 min.
GoTaq® DNA polymerase, 5 U/μL	50 mU/μL	8	Go to 6	Rep 25
		9	72 °C	10 min.
		10	4 °C	Hold

\*In 50 μL

Table 1: Final PCR Conditions. Final concentrations are given in a total final volume of 50 μL. 10x *Pfu* Ultra reaction buffer was from Stratagene, 600380-52; *Pfu* polymerase, was from Stratagene, 600380-51. GoTaq® Flexi DNA Polymerase was from Promega, M8291. These PCR conditions consistently generated a dense, sharp, 5.5 kb linear pACYCatpCROP product from the combination of two unique annealing temperatures and durations.

these two primers contained an extra GTP nucleotide at the 3' end, thereby giving rise to the extra GTP within the PCR product, pACYCatpCRop. To remove the extra base, primers were manufactured for site-directed mutagenesis and had the following sequences:

RopDelG (F):5' TC AAC GAA CTG GAC GCG GAT GAA CA 3'

RopDelG (R): 5' TG TTC ATC CGC GTC CAG TTC GTT GA 3'

A polymerase chain reaction, performed by Dixen Chen, using the site-directed mutagenesis primers RopDelG (F) and RopDelG (R), generated the appropriately-sized (5.5 kb) PCR product. The PCR product was gel-purified. High-efficiency transformation was completed using 5- $\alpha$ F'I<sup>q</sup> competent cells, according to manufacturer's specifications, with chloramphenicol on Luria-Bertani (LB) plus agar plates. Cells were incubated overnight at 37°C in a shaking incubator. Plasmid preparation was performed according to manufacturer's specifications, except that the DNA was eluted with water, not with EB buffer. The plasmid was sequenced at the Iowa State DNA Sequencing Facility (Ames, Iowa). The resulting sequence, presented in Figure 9, atpCRop DNA sequence, indicated that the inserted GTP nucleotide was successfully removed.

### **Expression of the Gamma-Rop Construct**

To facilitate biophysical studies, wild type rubrum chloroplast  $\alpha$ ,  $\beta$ , and spinach chloroplast  $\gamma$  ATP synthase subunits were over-expressed in BL21DE3(pLys) competent cells and purified according to previously published procedures [24 – 26].

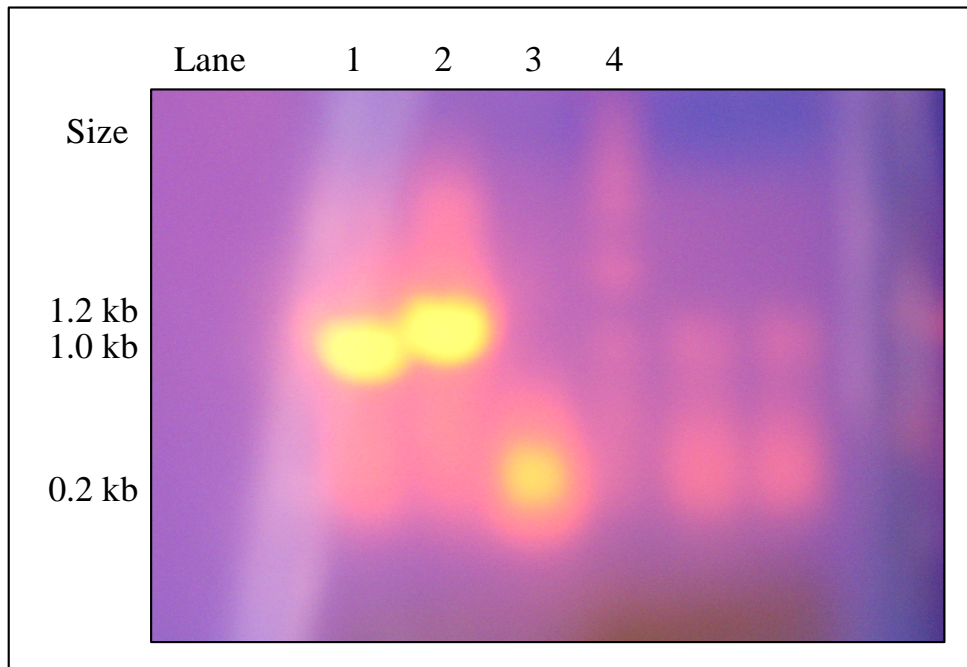


Figure 7: Agarose gel analysis of PCR products from the following reactions, where F stands for Forward and R stands for Reverse:

Lane 1: gamma (F) + gamma (R) with pACYCatpC (wild type), band size: ~1 kb;

Lane 2: gamma (F) + gamma (R) with pACYCatpCRop, band size: ~1.2 kb;

Lane 3: Rop (F) + Rop (R) with pACYCatpCRop, band size: ~200 bp;

Lane 4: 10 kb ladder (Bioline).

```

43 AAA AAC ACG CAG AAG ATC ACC GAA GCA ATG AAG CTC GTC GCC
85 GCC GCT AAA GTC CGC CGT GCG CAA GAA GCC GTC GTA AAC GGC
127 CGC CCC TTC TCG GAG ACT CTA GTC GAA GTT CTT TAC AAC ATG
169 AAT GAA CAG CTA CAG ACT GAG GAT GTT GAT GTT CCT CTG ACG
211 AAG ATT CGG ACG GTG AAG AAG GTG GCG TTG ATG GTG GTT ACC
253 GGC GAC CGT GGT CTT TGC GGC GGG TTT AAT AAT ATG TTG CTG
295 AAG AAG GCT GAG TCT AGG ATT GCT GAG CTT AAG AAG CTT GGT
337 GTT GAT TAT ACT ATT ATT AGT ATT GGA AAG AAA GGA AAC ACT
379 TAT TTT ATC CGG CGT CCT GAG ATT CCC GTC GAC AGG TAC TTC
421 GAC GGA ACA AAC CTA CCA ACC GCC AAA GAA GCA CAA GCC ATA
463 GCA GAC GAC GTC TTC TCC CTA TTC GTA AGC GAA GAA GTC GAC
505 AAA GTC GAA ATG CTC TAC ACA AAA TTC GTC TCT TTA GTA AAA
547 TCA GAC CCA GTA ATC CAC ACC CTA CTC CCC CTC TCA CCC AAA
589 GGA GAA ATT TGC GAC ATC AAT GGA AAA TGT GTC GAC GCA GCA
631 GAA GAC GAA CTC TTC CGT CTC ACA ACA AAA GAA GGT AAG

```

```

ROP ACC AAA CAG GAA AAA ACC GCC CTT AAC ATG GCC CGC TTT ATC
ROP AGA AGC CAG ACA TTA ACG CTG CTG GAG AAG CTC AAC GAA CTG
ROP G*GA CGC GGA TGA^ ACA GGC AGA TAT CTG TGA ATC GCT TCA CGA
ROP CCA CGC CGA TGA GCT TTA CCG CAG TTG CCT CGC TCG CTT CGG
ROP GGA TGA CGG TGA AAA CCT

```

670 CCT

```

673 AAC GGT AGA AAG AGA CAT GAT CAA AAC CGA AAC ACC AGC ATT
715 TTC CCC AAT TCT GGA ATT CGA ACA AGA TCC TGC TCA AAT TCT
757 CGA CGC TTT GCT TCC ATT ATA CTT AAA CAG TCA GAN TTT GAG
799 GGC TTT ACA AGA ATC ACT TGC TAG TGA ACT TGC TGC GAG GNA

```

Figure 8: Mutant atpCRop DNA sequence. The gamma DNA sequence is in green, the Rop N-terminal DNA sequence is in red, and the Rop C-terminal DNA sequence is in blue; the asterisk (\*) corresponds to the inadvertent GTP nucleotide at the junction of primers Rop28gamma and Rop34gamma. A carrot (^) denotes the premature stop codon.

Expression of the gammaRop mutant resulted in a protein slightly larger in size than the wild type gamma, visualized with SDS-PAGE, as indicated in Figure 10.

### **Conclusions and Implications for Further Research**

The inverse PCR extension method is commonly used for the introduction of nucleotide changes, for the insertion of small lengths of exogenous DNA into a gene or vector [19, 20], or in the deletion of >100 base pairs of a gene of interest with higher deletion efficiency than the overlapping primer method [21]. The insertion of the *rop* DNA into the *gamma* gene, an insert of 189 base pairs of foreign DNA, represents a novel application of this method, made possible using the multi-step PCR approach described in Table 1.

Optimal long primer inverse PCR required an initial round (step one) with low annealing temperature and short annealing duration because primers were required to anneal to approximately 21 bases of the gamma subunit sequence. During the second PCR step, the annealing temperature and duration were increased significantly because the primers were annealing to a DNA sequence that was complementary to the entire primer length (>100 base pairs). This two-step inverse PCR method resulted in a linear product that was successfully phosphorylated and ligated. The ligated construct was transformed into high-efficiency cloning cells then into over-expression cells for successful over-expression. One highly advantageous property of this inverse PCR technique was that it avoided inadvertent inclusion or omission of base pairs associated with restriction digestion methods, therefore reducing the

43 AAA AAC ACG CAG AAG ATC ACC GAA GCA ATG AAG CTC GTC GCC  
85 GCC GCT AAA GTC CGC CGT GCG CAA GAA GCC GTC GTA AAC GGC  
127 CGC CCC TTC TCG GAG ACT CTA GTC GAA GTT CTT TAC AAC ATG  
169 AAT GAA CAG CTA CAG ACT GAG GAT GTT GAT GTT CCT CTG ACG  
211 AAG ATT CGG ACG GTG AAG AAG GTG GCG TTG ATG GTG GTT ACC  
253 GGC GAC CGT GGT CTT TGC GGC GGG TTT AAT AAT ATG TTG CTG  
295 AAG AAG GCT GAG TCT AGG ATT GCT GAG CTT AAG AAG CTT GGT  
337 GTT GAT TAT ACT ATT ATT AGT ATT GGA AAG AAA GGA AAC ACT  
379 TAT TTT ATC CGG CGT CCT GAG ATT CCC GTC GAC AGG TAC TTC  
421 GAC GGA ACA AAC CTA CCA ACC GCC AAA GAA GCA CAA GCC ATA  
463 GCA GAC GAC GTC TTC TCC CTA TTC GTA AGC GAA GAA GTC GAC  
505 AAA GTC GAA ATG CTC TAC ACA AAA TTC GTC TCT TTA GTA AAA  
547 TCA GAC CCA GTA ATC CAC ACC CTA CTC CCC CTC TCA CCC AAA  
589 GGA GAA ATT TGC GAC ATC AAT GGA AAA TGT GTC GAC GCA GCA  
631 GAA GAC GAA CTC TTC CGT CTC ACA ACA AAA GAA GGT AAG

ROP ACC AAA CAG GAA AAA ACC GCC CTT AAC ATG GCC CGC TTT ATC  
ROP AGA AGC CAG ACA TTA ACG CTG CTG GAG AAG CTC AAC GAA CTG  
ROP GAC GCG GAT GAA CAG GCA GAT ATC TGT GAA TCG CTT CAC GAC  
ROP CAC GCC GAT GAG CTT TAC CGC AGT TGC CTC GCT CGC TTC GGG  
ROP GAT GAC GGT GAA AAC CTC

670 CTA

673 ACG GTA GAA AGA GAC ATG ATC AAA ACC GAA ACA CCA GCA TTT  
715 TCC CCA ATT CTG GAA TTC GAA CAA GAT CCT GCT CAA ATT CTC  
757 GAC GCT TTG CTT CCA TTA TAC TTA AAC AGT CAG ANT TTG AGG  
799 GCT TTA CAA GAA TCA CTT GCT AGT GAA CTT GCT GCG AGG

Figure 9: atpCRop DNA sequence. The gamma DNA sequence is in green, the Rop N-terminal DNA sequence is in red, and the Rop C-terminal DNA sequence is in blue.

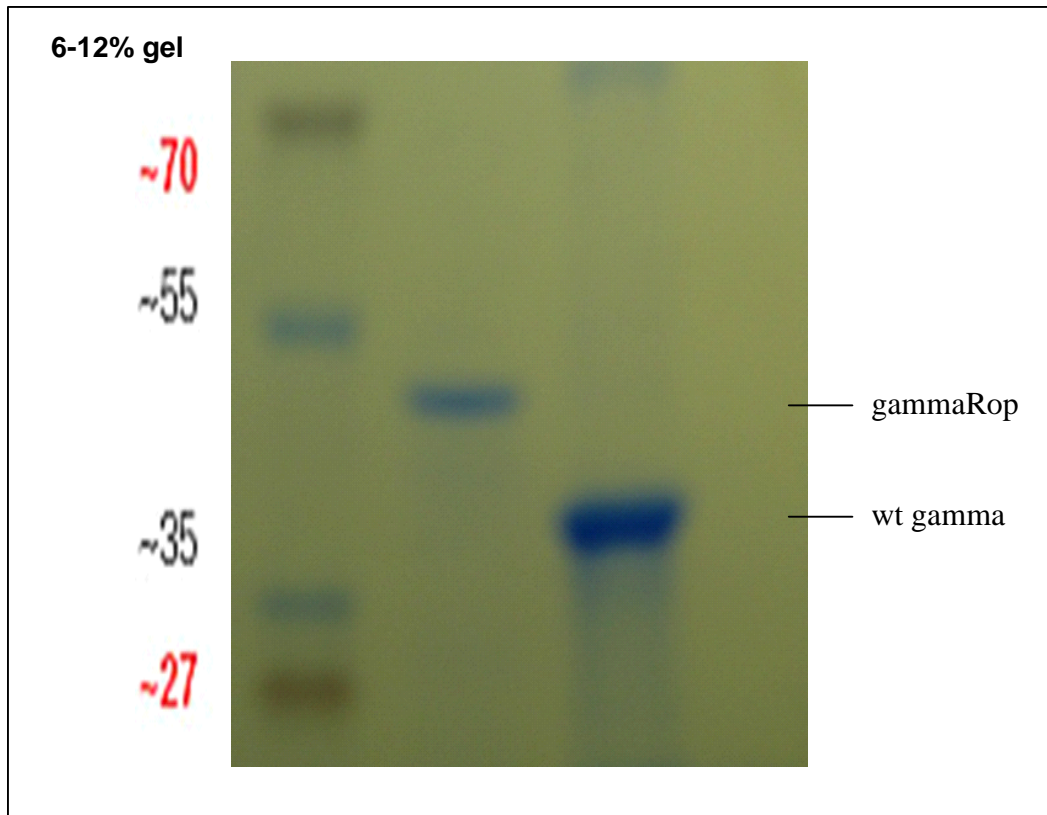


Figure 10: SDS-PAGE analysis of gammaRop. Inclusion bodies of wild type and gammaRop subunits were dissolved in SDS sample buffer and ~5-10  $\mu$ g of each subunit was subjected to SDS-PAGE on a 12 % NewPage gel. The wild type gamma subunit is approximately 35 kDa; the gammaRop mutant protein migrates as a protein that is approximately 7 kDa larger than the wild type gamma subunit as indicated by the standard proteins shown on the left side of the gel.

incidence of missense mutations. Also, the inverse PCR approach inserted the DNA sequence of interest in a single orientation, unlike traditional restriction digestion and ligation methods, where varying ratios and orientations of products are possible. The inverse PCR technique also avoids other problems associated with traditional cloning approaches, including difficulty digesting DNA using restriction digestion enzymes, ligating insert DNA into a template, and ensuring that the ligated product contains the sequence of interest in the proper insert:vector ratio.

This novel method resulted in the successful generation of a recombinant ATP synthase gamma subunit that has since been successfully assembled with the  $\alpha$  and  $\beta$  subunits (Mehta, Chen, Gao, and Richter, personal communication). The new assembly will be of considerable value in the analysis of  $\gamma$  subunit rotation and in the construction of nanodevices that are based on the rotational capability of the  $F_1$  molecule. The next step in this process is to engineer a site for attachment of metallic beads to the extended Rop armature within the gamma subunit for dark-field microscopic studies of the rotational kinetics and for further development of the ATP-driven electricity generator described earlier.

In conclusion, a novel method has been described for the direct incorporation of 189 bases of exogenous DNA into a specific location within the gene encoding the  $\gamma$  subunit of the chloroplast ATP synthase using a simple two-step PCR extension method. Because of its ease of use and advantages over traditional cloning techniques, we anticipate that the method will be valuable for a variety of applications requiring the insertion of long pieces of exogenous DNA into host DNA molecules.

## References

1. Nakamoto, R. K., Ketchum, C. J., Al-Shawi, M. K., Rotational Coupling in the F<sub>0</sub>F<sub>1</sub> ATP Synthase, *Annual Review of Biophysical and Biomolecular Structure*, **1999**, 28, 205 – 234.
2. Abrahams, J. P., Leslie, A. G., Lutter, R., Walker, J. E., Structure at 2.8 Å resolution of F<sub>1</sub>-ATPase from bovine heart mitochondria, *Nature*, **1994**, 370, 621 – 628.
3. Girault, G., Berger, G., Galmiche, J. M., Andre, F., Characterization of six nucleotide-binding sites on chloroplast coupling factor 1 and one site on its purified β subunit, *J. Biol. Chem.*, **1988**, 263, 14690 – 14695.
4. Boyer, P. D., The binding change mechanism for ATP synthase: Some probabilities and possibilities, *Biochim. Biophys. Acta*, **1993**, 1140, 215 – 250.
5. Boyer, P.D., The ATP synthase: A splendid molecular machine, *Annu. Rev. Biochem.*, **1997**, 66, 717 – 749.
6. Cross, R. L., The rotary binding change mechanism of ATP synthesis, *Biochim. Biophys. Acta*, **2000**, 1458, 270 – 275.
7. Gao, F., Lipscomb, B., Wu, I., Richter, M. L., In vitro assembly of the core catalytic complex of the chloroplast ATP synthase, *J. Biol. Chem.*, **1995**, 270, 9763 – 9769.
8. Milgrom, Y. M., Cross, R. L., Rapid hydrolysis of ATP by mitochondrial F<sub>1</sub>-ATPase correlates with the filling of the second of three catalytic sites, *Proc. Natl. Acad. Sci., U.S.A.*, **2005**, 102, 13831 – 13836.
9. Noji, H., Yasuda, R., Yoshida, M., Kinosita, Jr., K., Direct observation of the rotation of F<sub>1</sub>-ATPase, *Nature*, **1997**, 386, 299 – 302.
10. Yasuda, R., Noji, H., Yoshida, M., Kinosita, Jr., K., Itoh, H., Resolution of distinct rotational substeps by submillisecond kinetic analysis of F<sub>1</sub>-ATPase, *Nature*, **2001**, 401, 898 – 904.
11. Furuike, S., Hossain, M. D., Maki, Y., Adachi, K., Suzuki, T., Kohori, A., Itoh, H., Yoshida, M., Kinosita, Jr., K., Axle-less F<sub>1</sub>-ATPase Rotates in the Correct Direction, *Science*, **2008**, 319, 955 – 958.
12. Pu, J., Karplus, M., How subunit coupling produces the γ-subunit rotary motion in F<sub>1</sub>-ATPase, *Proc. Natl. Acad. Sci., U. S. A.*, **2008**, 105, 1192 – 1197.

13. Montemagno, C. D., Bachand, G. D., Constructing nanomechanical devices powered by biomolecular motors, *Nanotechnology*, **1999**, 10, 225 – 231.
14. Soong, R. K., Bachand, G. D., Neves, H. P., Olkhovets, A. G., Craighead, H. G., Montemagno, C. D., Powering an Inorganic Nanodevice with a Biomolecular Motor, *Science*, **2000**, 290, 1555 – 1558.
15. York, J., Spetzler, D., Hornung, T., Ishmukhametov, R., Martin, J., Frasch W. D., Abundance of *Escherichia coli* F<sub>1</sub>-ATPase molecules observed to rotate via single-molecule microscopy with gold nanorod probes, *Journal of Bioenergetics and Biomembranes*, **2007**, 39, 435 – 439.
16. Cesareni, G., Muesing, M. A., Polisky, B., Control of ColE1 DNA replication: The *rop* gene product negatively affects transcription from the replication primer promoter, *Proc. Natl. Acad. Sci., U.S.A.*, **1982**, 79, 6313 – 6317.
17. Lacatena, R. M., Banner, D. W., Castagnoli, L., Cesareni, G., Control of Initiation of pMB1 Replication: Purified Rop Protein and RNA I Affect Primer Formation In Vitro, *Cell*, **1984**, 37, 1009 – 1014.
18. Eberle, W., Pastore, A., Sander, C., Rösch, P., The structure of ColE1 rop in solution, *Journal of Biomolecular NMR*, **1991**, 1, 71 – 82.
19. Uccelli, A., Oksenberg, J. R., Jeong, M. C., Genain, C. P., Tombos, T., Jaeger, E. E. M., Giunti, D., Lanchbury, J., S., Hauser, S. L., Characterization of the TCRB Chain Repertoire in the New World Monkey *Callithrix jacchus*, *The Journal of Immunology*, **1997**, 158, 1201 – 1207.
20. Ochman, H., Gerber, A. S., Hartl, D. L., Genetic Applications of an Inverse Polymerase Chain Reaction, *Genetics*, **1988**, 120, 621 – 623.
21. Williams, M., Louw, A. I., Birkholtz, L-M., Deletion mutagenesis of large areas in *Plasmodium falciparum* genes: a comparative study, *Malaria Journal*, **2007**, 6, 64 - 72.
22. Cheng, S., Fockler, C., Barnes, W. M., Higuchi, R., Effective amplification of long targets from cloned inserts and human genomic DNA, *Proc. Natl. Acad. Sci. U. S. A.*, **1994**, 91, 5695 – 5699.
23. Sokolov, M., Lu, L., Tucker, W., Gao, F., Gegenheimer, P. A., Richter, M. L., The 20 C-terminal Amino Acid Residues of the Chloroplast ATP Synthase  $\gamma$  Subunit Are Not Essential for Activity, *The Journal of Biological Chemistry*, **1999**, 274, 20, 13824 – 13829.

24. Richter, M. L., Samra, H. S., He, F., Giessel, A. J., Kuczera, K. K., Coupling Proton Movement to ATP synthesis in the Chloroplast ATP Synthase, *Journal of Bioenergetics and Biomembranes*, **2005**, 37, 467 – 473.
25. Samra, H. S., Gao, F., He, F., Hoang, E., Chen, A., Gegenheimer, P. A., Berrie, C. L., Richter, M. L., Structural Analysis of the Regulatory Dithiol-containing Domain of the Chloroplast ATP Synthase  $\gamma$  Subunit, *The Journal of Biological Chemistry*, **2006**, 281, 41, 31041 – 31049.
26. He, F., Samra, H. S., Johnson, E. A., Degner, N. R., McCarty, R. E., Richter, M. L., C-Terminal Mutations in the Chloroplast ATP Synthase  $\gamma$  Subunit Impair ATP Synthesis and Stimulate ATP Hydrolysis, *Biochemistry*, **2008**, 47, 836 – 844.
27. Davidson, R. C., Blankenship, J. R., Kraus, P. R., Berrios, M. D., Hull, C. M., D'Souza, C., Wang, P., Heitman, J., A PCR-based strategy to generate integrative targeting alleles with large regions of homology, *Microbiology*, **2002**, 148, 2607 – 2615.